Effects of thermal annealing on SEBS/MWCNTs temperature-sensitive nanocomposites for the measurement of skin temperature.

N. Calisi[1*], P. Salvo[1,2], B. Melai[1], C. Paoletti[1], A. Pucci[1], F. Di Francesco[1]

[1] Department of Chemistry and Industrial Chemistry, University of Pisa, Via Moruzzi 13, 56124, Pisa, Italy.

[2] Institute of Clinical Physiology, National Council of Research (IFC-CNR), Via Moruzzi 1, 56124, Pisa, Italy.

* Corresponding author, Tel: +39 050 2219001, email: nicola.calisi@dcci.unipi.it

Abstract

The monitoring of skin temperature is essential for many applications, especially in sport and medicine. In this work, a flexible and wearable temperature sensor was obtained thanks to the controlled incorporation of multi-walled carbon nanotubes (MWCNTs) in an elastomeric matrix based on a poly(b-styrene-b-(ethylene-co-butene)-b-styrene) matrix. Thermal annealing at 155°C for 4 hours decreased the percolation threshold of the nanocomposite by about 40% thanks to the strong modification of the copolymer phase structure, which provided a more effective percolative network. The proposed temperature sensor prototype showed a very high linearity (R^2 = 0.9987) and reproducibility (standard deviation < 1%) for temperature variations within the physiological regime.

Keywords

Carbon nanotubes, nanocomposite, temperature sensor, annealing.

1. Introduction

Being able to monitor skin temperature is important in many fields. In sports training the temperature of the skin is correlated with the intensity of the exercise so measuring the temperature during an exercise can help the trainer to match the training to the athlete [1]. Temperature monitoring is also important in medicine, as the temperature of the human body is correlated with many diseases. For example, the formation of some wounds (e.g. diabetic foot ulcers and decubitus ulcers) is pre-empted by a decrease in skin temperature [2, 3], whereas inflammation can increase the temperature of an open wound. In many medical applications, temperature sensors are required to be small sized and wearable to be beneficial [4, 5].

Since their discovery [6], carbon nanotubes (CNTs) have become an attractive material for the scientific community due to their high aspect ratio and appealing properties such as an extremely high tensile modulus (640 GPa to 1 TPa) and tensile strength (155-180 GPa), as well as high thermal (theoretically > 600 W/(m K)) and electrical conductivities (10^{-6} Ω cm^{-1}) [7]. CNTs can either be single- or multi-walled (SWCNTs and MWCNTs, respectively), i.e. they consist of a single cylinder with a typical diameter of 1-2 nm or multiple concentric cylinders. In the latter, the intertube distance is similar to the interlayer distance between two graphene sheets in graphite (0.34 nm) [8]. SWCNTs can show a metal-like or semiconductor-like behaviour depending on the chirality, whereas MWCNTs have a semiconductor nature [9].

These excellent properties make carbon nanotubes potentially useful in many applications such as transparent electrodes, electrodes for lithium ion batteries, capacitors, contacts in organic field effect transistors, fuel cells, filters, and sensors [10].

CNTs can also be used to improve the mechanical properties of other materials, for example to reinforce polymers and produce high strength, lightweight and high-performance composites [11]. The thermal and electrical properties of SWCNT-polymer composites are significantly enhanced by magnetic alignment during processing [12].

Today polymers loaded with CNTs are among the most interesting nanocomposites. A nanocomposite has physical and chemical properties which are very different from the starting material because the large surface area of CNTs promotes a strong interaction with the matrix. A fine dispersion of the nanoparticles is essential to obtain nanocomposites with optimum properties. Unfortunately, the strong Van der Walls interactions among single CNTs due to the large surface area hamper their dispersion. In addition, nanotubes are insoluble in most common organic and inorganic solvents, so that ultrasonication or high-speed shearing have to be used to obtain CNT/polymer nanocomposites. These treatments tend to damage CNTs, dramatically shortening their length and introducing structure defects [13]. Surfactants can be used to increase the solubility of CNTs in common solvents [14].

In a previous study, we manufactured a temperature sensor based on a MWCNT and poly(b-styrene-b-(ethylene-co-butene)-b-styrene) (SEBS) nanocomposite by ultrasonicating MWCNTs in toluene and adding the centrifuged dispersion to a SEBS solution in toluene [15]. The SEBS structure, which is rich in benzene rings, made this polymer at the same time act as a surfactant, thus stabilizing the suspension thanks to the strong interaction with MWCNTs, and as a supporting matrix with good filming properties. Electrically conductive and temperature-sensitive nanostructured films were then obtained by drop casting the dispersion onto a Kapton™ film supporting gold electrodes.

In another study, we correlated the amount of dispersed MWCNTs and the resistance of the films to the ultra-sonication time [16]. Determination of the length distribution enabled the damage caused to MWCNTs by the dispersion process to be quantified, and alkyl-functionalized MWCNTs (f-MWCNTs) were tested to improve the quality of the dispersion. Higher amounts of dispersed material were obtained with f-MWCNTs, also with a shorter sonication time. The sensitivity to temperature of the films was tested between 25 °C and 50 °C. In this range, the temperature was increased with 5 °C steps and the electrical resistance of the film was recorded after reaching a stable temperature. The optimization of SEBS/MWCNTs and SEBS/f-MWCNTs films improved the sensitivity during the first heating process but unfortunately there was a dramatic drop in sensitivity after the first heating cycle.

Block copolymers such as SEBS are organized into ordered microdomains [17]. Different deposition methods and drying procedures can lead to microdomains with different shapes and characteristics. A temperature increase may cause a transition between two different conformations of the polymer microdomains by providing enough kinetic energy to turn a poorly ordered polymer into a more stable conformation [18]. SEBS shows two different kinds of microdomains, namely styrene domains with a high Young's modulus (24 ± 3.1), and poly(ethylene-co-butene) domains with a small Young's modulus (6.4 ± 0.3) [19]. Three different transitions of the microdomain conformations in SEBS have been reported, namely the order-order transition (OOT) at 155 °C which turns cylinders into spheres, the lattice disordering transition (LDT) at 170 °C, and the order-disorder transition (ODT) at 202 °C [20]. Even if the range of temperature used to test our sensor

was far from the lowest reported transition temperature, we speculated that the thermal instability of the polymeric matrix may be related to its limited reproducibility.

In this study, we evaluate the effect of a thermal treatment on nanocomposite films based on SEBS/MWCNT mixtures. The aim of this treatment is the thermal and dimensional stabilization of the polymeric matrix and the percolative network so that temperature sensors with improved reproducibility over multiple heating cycles can be obtained.

2. Materials and Methods

2.1. Materials and Instrumentation

Multi-walled carbon nanotubes (MWCNTs, Baytubes C155 P) were used as received. These nanotubes are vapour grown and typically consist of 3 - 15 graphitic layers wrapped around a hollow 4 nm core. Typical diameters range from 13 to 16 nm, and the lengths are between 1 and 10 μm. The density is approximately 1.4–1.6 g/cm^3.

Poly(b-styrene-b-(ethylene-co-butene)-b-styrene) (SEBS, Europrene Sol TH 212) was supplied by Polimeri Europa and used as received. This tri-block copolymer (M_W= 65–70 X 10^3, M_W/M_n = 1.03–1.11) consists of 19% units of styrene, 32.4% units of 1,2-butadiene and 48.6% units of 1,4-butadiene respectively. The ethylene-co-butene (EB) block has a glass transition temperature (Tg) of about -57 °C, whereas polystyrene blocks have a glass transition temperature of about 80 °C. All other chemicals were purchased from Sigma Aldrich and used as received.

Differential scanning calorimetry (DSC) analyses were performed under nitrogen flux (80 mL/min) with a Mettler-Toledo/DSC 822e equipped with a cooling system. The calibration was performed with Zinc and Indium. Heating and cooling thermograms were carried out at a standard rate of 10 °C/min.

The morphology of the SEBS/MWCNTs solid composites were examined with a multimode atomic force microscope (AFM, Veeco Metrology, Inc.) equipped with E and J piezoelectric scanners (Veeco Metrology, Inc.). The instrument was connected to Nanoscope IV controller (Veeco Metrology, Inc.) and a signal direct access module connected to TDS 2004B oscilloscope (Tektronix, Inc., Beaverton, OR).

Thermogravimetric analysis (TGA) was carried out by a Mettler Toledo Starc System (TGA/SDTA851^e). Samples were heated from 25 °C to 600 °C at 10 °C/min under a nitrogen flow, and from 600 to 900 °C under an air flow.

The ATR/FT-IR spectra of nanocomposite films were collected by a Perkin-Elmer Spectrum GX FT-IR instrument equipped with a MIRacle^{TM} ATR with a germanium crystal (IR penetration about 0.66 μm) and interfaced with a personal computer running the Spectrum v3.02 software.

2.2. Methods

Dispersions were obtained with a similar method to that described in [16]. A SEBS stock solution (0.4 g/L) was prepared by dissolving the polymer in toluene, then 1.2 g of MWCNTs (same weight as the polymer) were added to a 3 mL aliquot and sonicated at full power (Hielscher UP 400 S tip

sonicator, 400 W) at 24 kHz for 5 minutes. During sonication, the dispersion was cooled using a water-ice bath to reduce the evaporation of the solvent. The resulting dispersions were centrifuged at 4000 rpm for 30 min and then filtered to remove the residual MWCNT agglomerates. Nanocomposite films were obtained by casting 10 µL of the SEBS/MWCNT dispersions onto either Petri dishes or on sensor supports (Figure 1) purchased from Cad Line (Pisa, Italy). These substrates were made in polyimide (Kapton®, thickness 50 µm), which was selected due to its flexibility, chemical inertness, and low permeability to water and vapour. Tracks were prepared by photolithography on copper, and then electroplated with nickel and gold to fabricate the electrodes (dimensions: length 7 mm, width 1 mm, distance 2 mm; thickness of copper 35 µm, nickel 3.0 µm, gold 1.2 µm). An Agilent U1242A digital multimeter was used to measure the electric conductivity. The measurements were carried out on dried films obtained after solvent evaporation at room temperature for 24 hours.

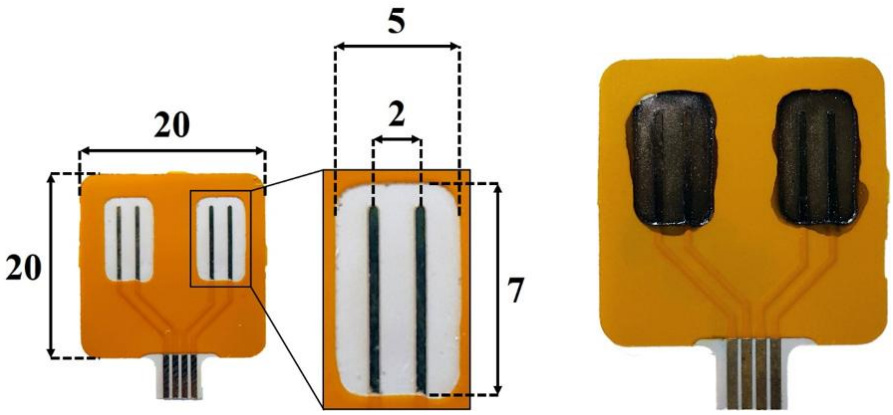

Figure 1: (Left) The Kapton® support, measurements are in millimetres. (Right) A temperature sensor prototype.

2.3.Annealing

For the mechanical stabilization of the nanocomposite, a thermal treatment was performed on dried films. The film was heated at 155 °C in an oven for 4 hours, after which, the film was removed from the oven and cooled at room temperature.

2.4.Sensors test

The experimental set-up used to test the sensors at a controlled temperature consisted of two aluminium plates heated by two mica heaters. The heaters were controlled by a Jumo 316 dTRON controller. The system was enclosed in a box made with Teflon® to isolate it from the environment. The temperature was controlled with a precision Pt100 probe (RS Pro, 611-7794).

3. Results and Discussion

The electrical resistance of the films, obtained by drop-casting aliquots of SEBS/MWCNT dispersions, was investigated in the range of 20–50 °C to explore their potential for the

development of sensitive, stable, and reproducible skin temperature sensors.
First, a DSC study was carried out to determine the thermal behaviour of the polymer within the temperature range investigated.

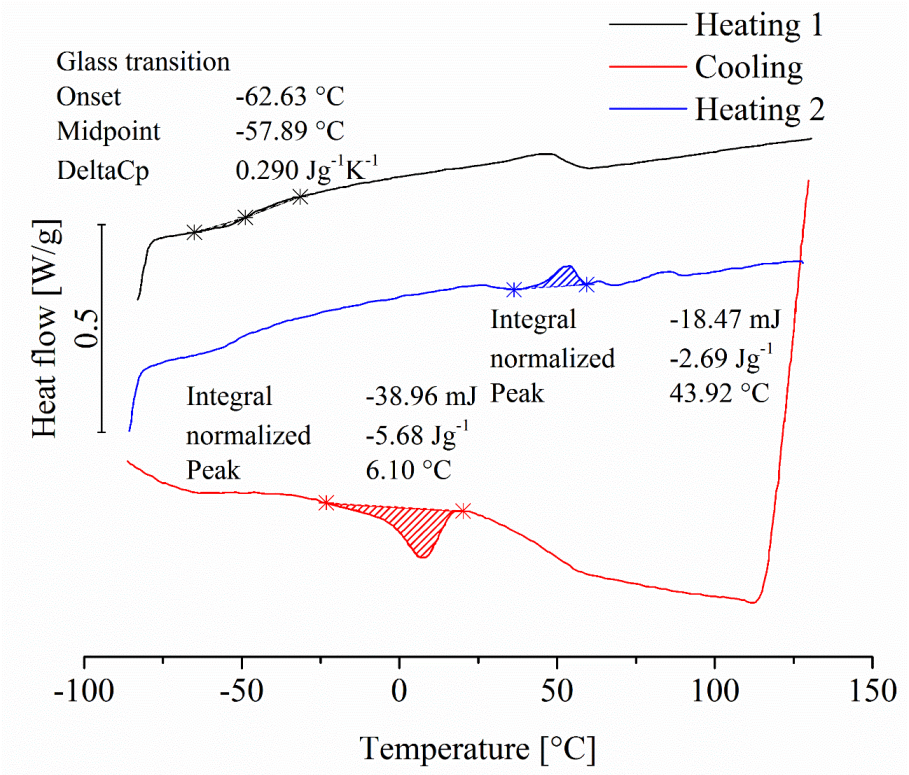

Figure 2: Analysis of a SEBS sample: the upper black line is the first heating, the lower red line is the cooling, and the central blue line is the second heating.

Figure 2 highlights that the transition temperature of the hydrogenated ethylene-co-butene (EB) block is 44 °C. This transition probably leads to a significant modification in the nanocomposite matrix and consequently to a change in the topology of the percolation network. The DSC analysis showed the EB block glass-transition in the first heating (upper black line), which was identified at -62 °C. In the second heating (central blue line) the melting of the EB block was clearly visible at about 44 °C and the glass transition temperature of the styrene block was visible at about 80 °C. The crystallization of the EB block at about 6 °C was identified in the cooling (bottom red line). This process occurs at a temperature lower than the melting point. This could explain the high variation in the resistance of the nanocomposite film between the first and the second heating observed in our previous studies [14, 15]. In the sensor experiment, after the first heating, the device was cooled down to 25 °C and then the second heating started again from 25 °C to 50 °C. In this temperature range, the EB block did not crystallize, thus strongly influencing the sensor response within this temperature range.

The structure of the polymer and the percolation network were investigated using AFM analysis. The SEBS/MWCNT nanocomposite film was obtained with an initial ratio of 1:4 (ratio between MWCNTs and SEBS) before the sonication process and the centrifugation of the dispersion. The scan was acquired in the same zone of the nanocomposite film before and after heating the sample to 50 °C. The sample was heated directly on the AFM instrument thanks to a heating sample support. Figure 3 a) and b) show the AFM scans before and after the heating, respectively.

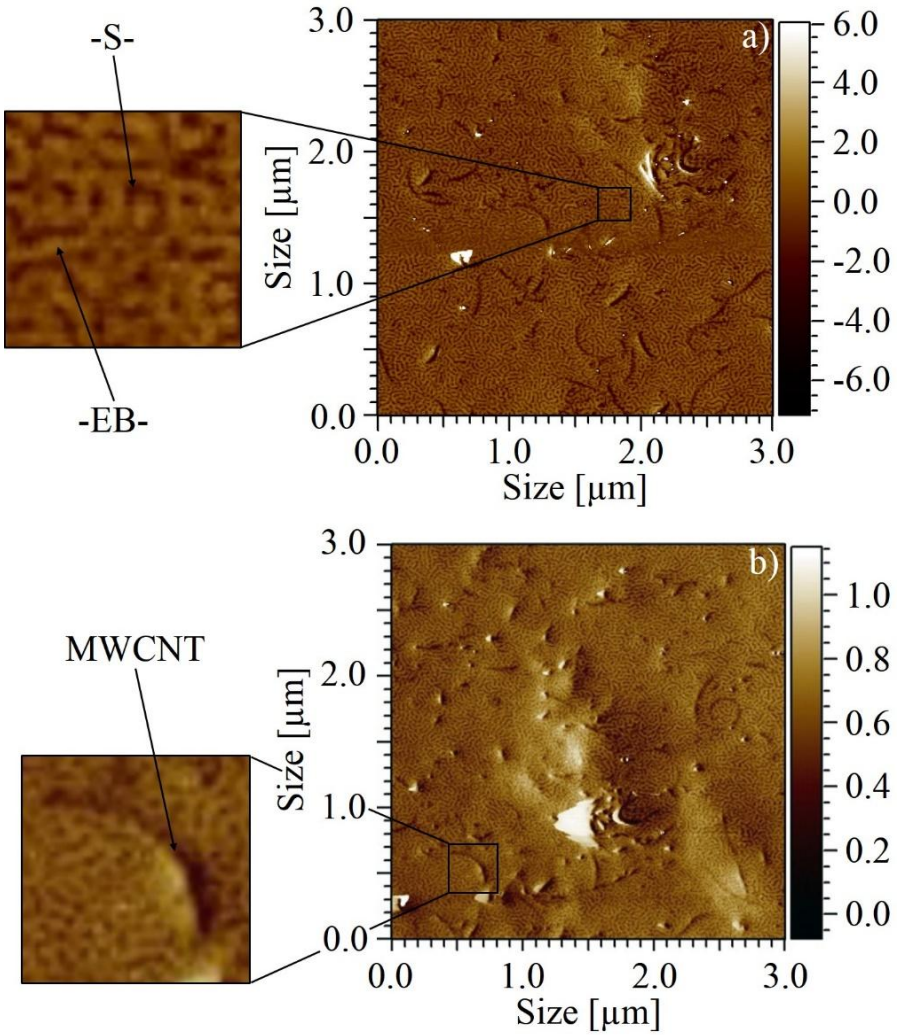

Figure 3: AFM phase scans of a SEBS/MWCNT film: a) AFM scan of the untreated film; b) AFM scan after the heating of the film to 50 °C. Two zooms showing the microdomain conformation (upper) and of a MWCNT (lower) are reported in the boxes.

The AFM phase scans were used to analyse the morphology of the nanocomposite film. Figure 3 shows the hardness from hard levels (black) to soft levels (white). The AFM scans also show that the SEBS microdomains before and after the heating were in the conformation of unaligned worm-like cylinders. The dark cylinders are the polystyrene domains (-S-), while the light cylinders are the -EB- domains. The big dark worms are the MWCNTs.

The AFM scans show that the conformation of the microdomains of the polymer did not change after heating to 50 °C. However, a comparison between Figures 3a and 3b reveal a significant change in the distribution of the MWCNTs, so it seems that such temperature increase can modify the topology of the percolation network. The conformation of the microdomains of the block copolymer is dramatically affected by the temperature [20]. To obtain a stable percolation network, an annealing treatment at 155 °C for 4 hours was performed on the nanocomposite films. This temperature is over the order-order transition (OOT) at 155 °C which turns cylinders into spheres

and possibly enables the kinetical stabilization of the polymeric matrix. A higher temperature can damage the substrate and cannot be applied to our sensors.

The same annealing at 155 °C for 4 hours was carried out on a SEBS sample. After this treatment a DSC analysis was performed on non-annealed and annealed SEBS samples to investigate whether the thermal properties of the polymer changed after the annealing (Figure 4).

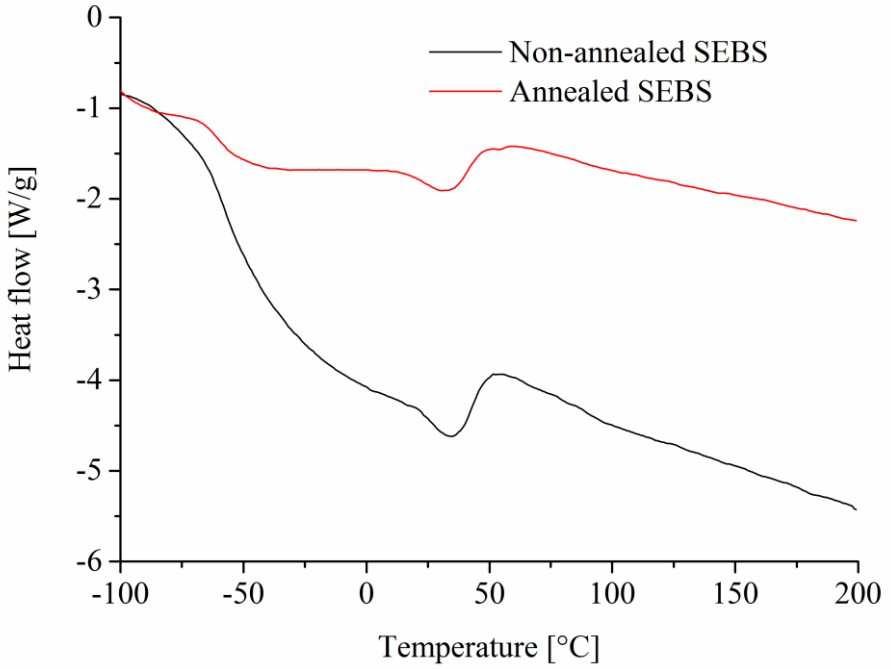

Figure 4: DSC analysis of non-annealed (black trace) and annealed (red trace) SEBS.

Figure 4 shows that, after the annealing of the polymer, the heat absorbed for the EB block melting decreased from -0.6805 W/g to -0.4593 W/g. Notably, after the annealing process, a small number of SEBS flakes changed colour and turned from white flakes to yellow melted balls. An ATR/FT-IR analysis was performed on both samples (white flakes and yellow melted balls) to investigate the differences between the two forms of SEBS (Figure 5).

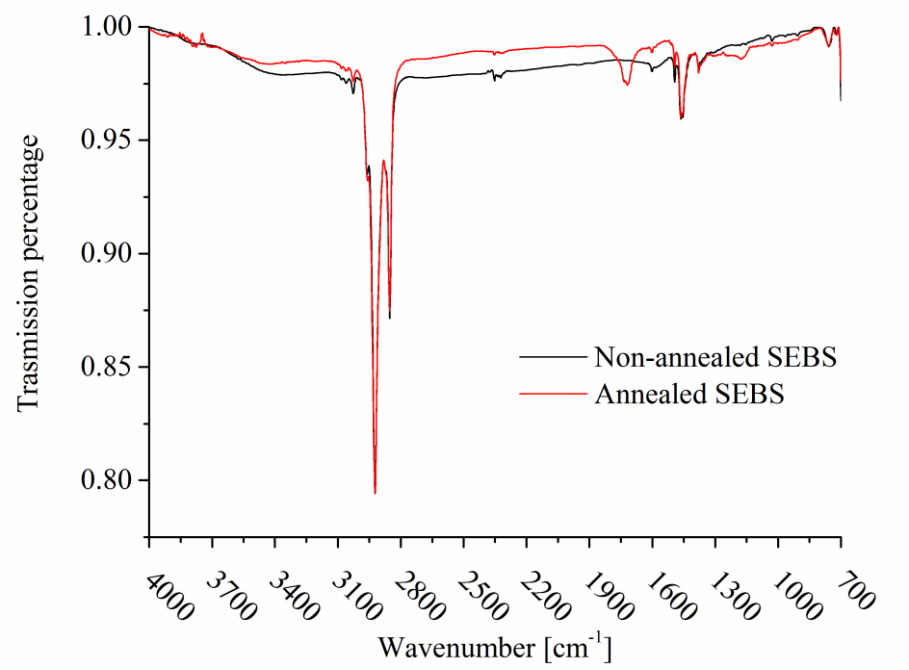

Figure 5: ATR/FT-IR spectrum of non-annealed and annealed SEBS sample.

Figure 5 shows an increase in the number of carbonyl groups after the annealing, in particular a peak of the aliphatic aldehydes at 1720 cm^{-1}. This enhancement suggests that some oxidised processes had occurred on the EB block after the annealing. This phenomenon has been reported in numerous papers regarding olefinic polymers [21, 22] and possibly affects the crystallization degree of the polymer [23].

An AFM scan was performed on the nanocomposite to investigate the conformation of the microdomains of the polymer after the thermal treatment (Figure 6). The SEBS/MWCNT nanocomposite film was obtained with an initial ratio of 1:4 (ratio between MWCNTs and SEBS) before the sonication and the centrifugation of the dispersion.

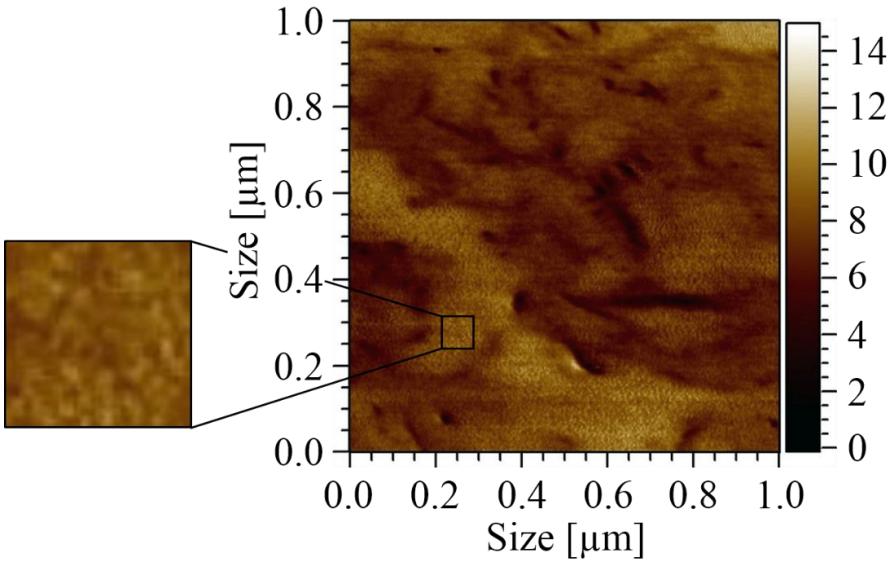

Figure 6: AFM phase scan of a SEBS/MWCNT film after a thermal treatment.

The AFM phase scan showed that microdomains change from a worm-like shape to a spherical conformation. Our analysis is in agreement with the literature which supports the evidence of an order-order transition at 155 °C from ordered worms to ordered spheres [20]. The transition of the microdomain of the polymeric matrix can give a higher thermal and dimensional stability to the film. In addition, a decrease in the number of MWCNTs on the surface of the film was observed. This can be explained by the deepening of MWCNTs on the film, which is further confirmed by the decrease in the percolation threshold.

The percolation thresholds of the SEBS/SWCNT nanocomposite films with different amounts of MWCNTs were evaluated at 25 °C, before and after the thermal treatment (Figure 7). The nanocomposite films were obtained by diluting the stock dispersion with a SEBS solution in toluene. The final SEBS/MWCNT ratio was evaluated on a dried nanocomposite by TGA analysis. Nanocomposite films were finally obtained by drop casting the dispersion onto the sensing substrate. The electrical resistances as a function of the frequency were acquired for the nanocomposites, before and after annealing at 155 °C for 4 hours.

The electrical resistance of materials composed of conductive and dielectric phases and depends on frequency, f, as the conductivity σ is proportional to ω^n, where $\omega = 2\pi f$ and $0.6 < n < 1$ [24]. In this study, we decided to focus on a frequency interval lower than 20 KHz, which is already much higher than the typical default frequency of 1 KHz used by commercial multimeters. Our aim was to obtain a material with a constant conductivity of at least up to 20 KHz in order to avoid the non-linear dependence of temperature on frequency. Figures 6a and 6b show the variation in resistance versus frequency for SEBS/SWCNT nanocomposite films before and after annealing, respectively. For the nanocomposites with low MWCNT loadings, the resistance decreased exponentially with frequency, which is a typical characteristic of insulating materials. Conversely, when the MWCNT content reaches the percolation threshold, the resistance is independent of the frequency.

In our tests, the annealing procedure decreased the percolation threshold from about 11 w/w % (Figure 7a) to about 7 w/w % (Figure 7b), possibly due to the formation of a more effective percolative MWCNT network within the SEBS matrix.

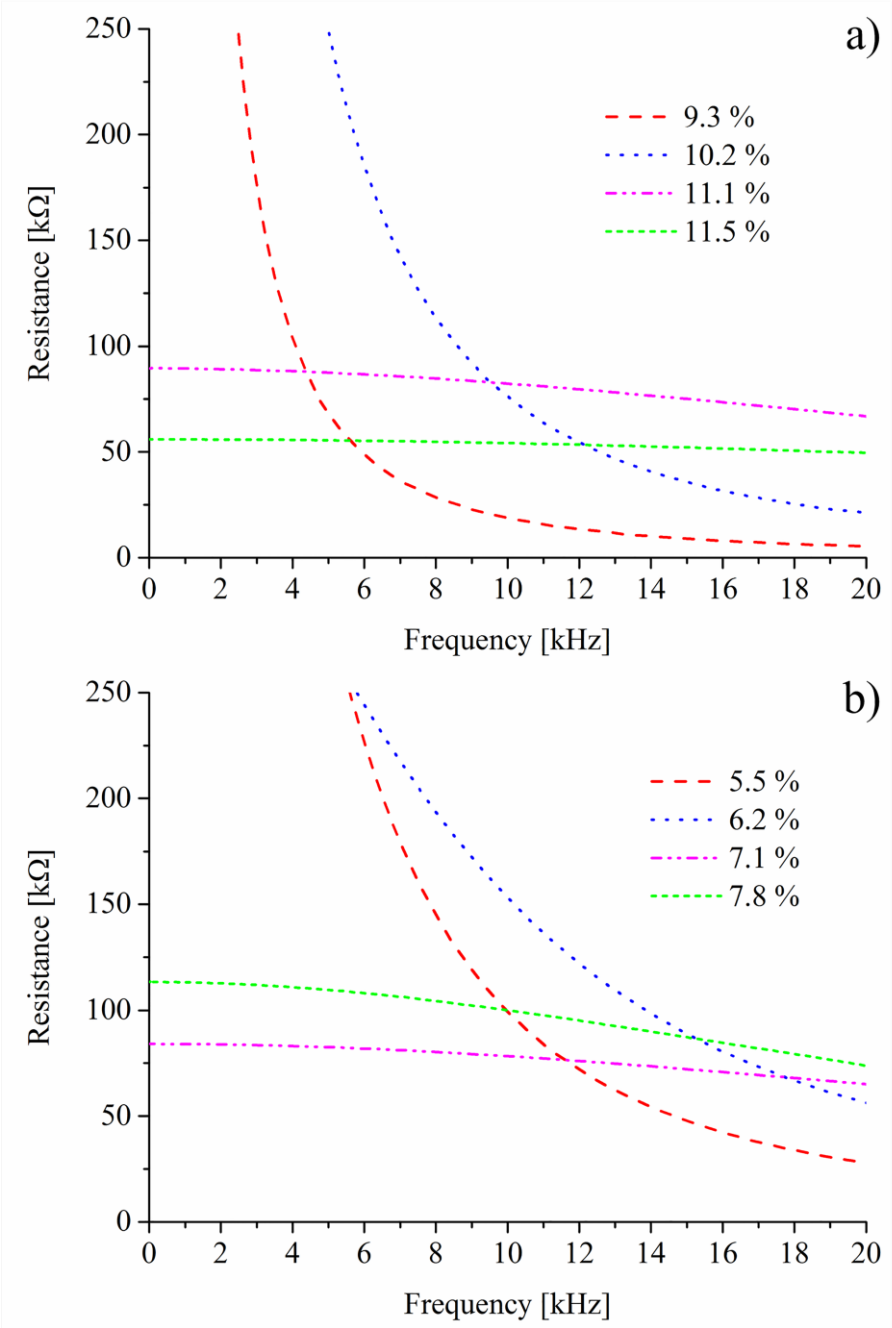

Figure 7: Electrical resistance of nanocomposite films with different SEBS/MWCNT ratios as a function of frequency:
a) non-annealed films: the percolation threshold is between 10.2 w/w % and 11.1 w/w % of MWCNT;
b) annealed films: the percolation threshold is between 6.2 w/w % and 7.1 w/w % of MWCNT.

A sensor made with an annealed nanocomposite film was then tested to verify our hypothesis concerning the increased stability of the film after treatment (Figure 8). This sensor was obtained depositing a dispersion with about 7 % w/w of MWCNTs. The amount of MWCNTs in the nanocomposite film was decreased to be near to the percolation threshold to reach the maximum sensitivity toward temperature changes.

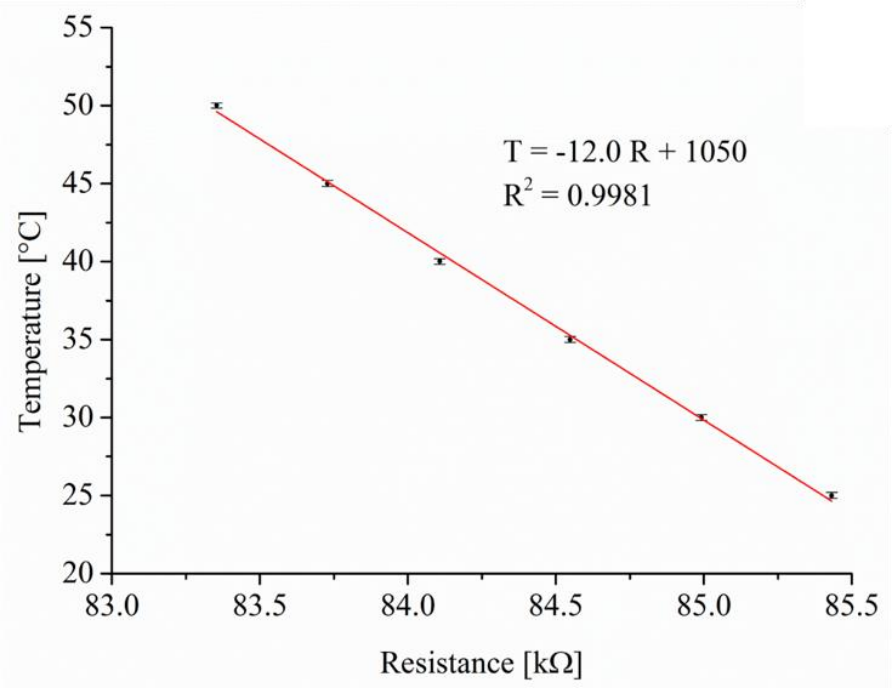

Figure 8: Calibration curve of a temperature sensor based on a SEBS/MWCNT nanocomposite (7 w/w %) after annealing at 155 °C for 4 hours.

Figure 8 reports the calibration curve of the sensor obtained after the nanocomposite had been annealed. Each point on the graph is the average of five consecutive measurements. This sensor shows a very good linearity and a very high repeatability. The sensitivity of the sensor, as shown by the function of the calibration curve, is about 100 Ω for each degree Celsius.

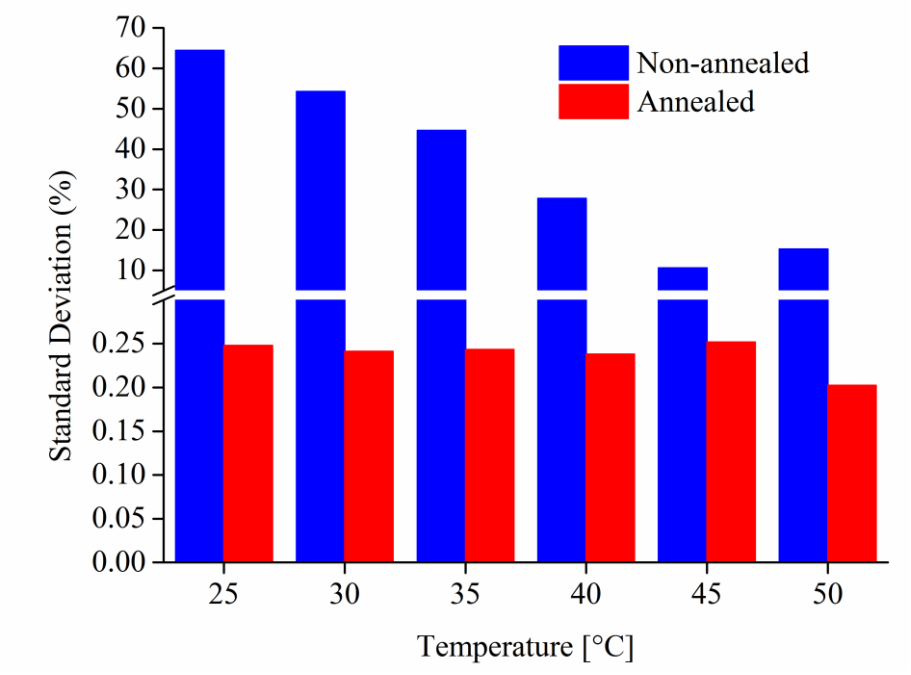

Figure 9: Comparison between percentage standard deviation of a non-annealed sensor (15 w/w %) and an annealed sensor (7 w/w %).

In Figure 9 reports the percentage standard deviation (%SD) versus temperature for the prepared sensors (15 w/w % of MWCNT in the non-annealed sensor and 7 w/w % in the annealed sensor) before and after the annealing process in order to evaluate the improvement obtained with the annealing process. The data show that the %SD decreased and the reproducibility improved after the film had been annealed. Before annealing, the %SD was very high in all the temperature intervals and decreased by 10% maximum when the temperature increased. After annealing, the %SD was lower than 0.25 %.

Figure 8b shows the calibration curve for the sensor. The linearity and the reproducibility increased compared with the non-annealed sensors, whereas the sensitivity decreased. The average accuracy of the sensor improved from ± 5 °C before annealing to ± 1 °C after annealing.

Conclusion

The effect of a thermal annealing on nanocomposite films based on SEBS/MWCNT mixtures was investigated. We had proposed a temperature sensor based on such material in previous studies which suffered from a drop in sensitivity after the first measurement cycle. In the present study, we hypothesized that a thermal treatment could modify the microdomain structure of the polymeric matrix and provide a higher thermal and dimensional stability to the film, thus improving the stability of the sensor over time and repeated measurement cycles.

DSC analysis highlighted the melting of the ethylene-butene block at a temperature of about 44 °C, so within our range of interest for the measurement of skin temperature, which could be responsible for a modification of the topology of the MWCNT network within the nanocomposite. Such modification was actually observed thanks to AFM scans after heating at 50 °C, even if the conformation of the microdomains was not affected. The thermal annealing at 155°C for 4 hours led to a remarkable rearrangement of the microdomain structure, whose shape changed from a worm-like to a spherical conformation in accordance to literature. The variation of the copolymer phase structure also decreased the percolation threshold of the nanocomposite by about 40%, from about 11 w/w % to about 7 w/w %. An ATR/FT-IR analysis showed that the annealing caused some minor oxidation processes of the polymer.

The test of a temperature sensor prototype showed a remarkable improvement in reproducibility (standard deviation < 1%) compared to previous achievements and very high linearity (R^2 = 0.9987). We believe that our results demonstrate the trueness of our hypothesis and pave the way for further improvements in the development of low cost and wearable sensors for the measurement of skin temperature.

Acknowledgement

This work was partially supported by the EU-funded FP7 ICT-317894 SWAN-iCare project.

References

[1] Z. J. Schlader, S. E. Simmons, S. R. Stannard, T. Mündel, European Journal of Applied Physiology, “Skin temperature as a thermal controller of exercise intensity”, 2011, 111, 1631-1639.

[2] D. G. Armstrong, L. A. Lavery, The journal of foot and ankle surgery, "Monitoring neuropathic ulcer healing with infrared dermal thermometry", 1996, 35, 4, 335-338.

[3] D. G. Armstrong, K. Holtz-Neiderer, C. Wendel, M. J. Mohler, H. R. Kimbriel, L. A. Lavery, The American Journal of Medicine, "Skin temperature monitoring reduces the risk for diabetic foot ulceration in high-risk patients", 2007, 120, 1042-1046.

[4] A. D. Harper Smith, D. R. Crabtree, J. L. J. Bilzon, N. P. Walsh, Physiological Measurement, "The validity of wireless iButtons® and thermistors for human skin temperature measurement", 2010, 31, 95-114.

[5] W. D. van Marken Lichtenbelt, H. A. M. Daanen, L. Wouters, R. Fronczek, R. J. E. M. Raymann, Natascha M. W. Severens, E. J. W. Van Someren, Physiology & Behavior, "Evaluation of wireless determination of skin temperature using iButtons", 2006, 88, 489-497.

[6] S. Iijima, Letters to nature, "Helical microtubules of graphitic carbon", 1991, 354, 56-58.

[7] M. Moniruzzaman, K. I. Winey, Macromolecules, "Polymer Nanocomposites Containing Carbon Nanotubes", 2006, 39, 5194-5205.

[8] P. M. Ajayan, Chemical Reviews, "Nanotubes from carbon", 1999, 99, 7, 1787-1799.

[9] P. R. Bandaru, Journal of Nanoscience and Nanotechnology, "Electrical properties and applications of carbon nanotube structures", 2007, 7, 1-29.

[10] J. M. Schnorr, T. M. Swager, Chemistry of Materials, "Emerging applications of carbon nanotubes", 2011, 23, 646-657.

[11] Z. Spitalskya, D. Tasis, K. Papagelis, C. Galiotis, Progress in Polymer Science, "Carbon nanotube–polymer composites: chemistry, processing, mechanical and electrical properties", 2010, 35, 357-401.

[12] F. F. Komarov, A. M. Mironov, Physics and chemistry of solid state, "Carbon nanotubes: present and future", 2004, 5, 3, 411-429.

[13] K. L. Lu, R. M. Lago, Y. K. Chen, M. L. H. Green, P. J. F. Harris, S. C. Tsang, Carbon, "Mechanical damage of carbon nanotubes by ultrasound", 1996, 18, 1089-1099

[14] X.-L- Xie, Y.-W. Mai, X.-P. Zhou, Materials Science and Engineering R, "Dispersion and alignment of carbon nanotubes in polymer matrix: a review", 2005, 49, 89-112.

[15] G. Matzeu, A. Pucci, S. Savi, M. Romanelli, F. Di Francesco, Sensors and Actuators A: Physical, "A temperature sensor based on a MWCNT/SEBS nanocomposite", 2012, 178, 94-99.

[16] N. Calisi, A. Giuliani, M. Alderighi, J. M. Schnorr, T. M. Swager, F. Di Francesco, A. Pucci, European Polymer Journal, "Factors affecting the dispersion of MWCNTs in electrically conducting SEBS nanocomposites", 2013, 49, 1471-1478.

[17] C. D. Han, J. Kin, J. K. Kim, Macromolecules, "Determination of the order-disorder transition temperature of block copolymers", 1989, 22, 383-394.

[18] R. Krishnamoorti, M. A. Modi, M. F. Tse, H.-C. Wang, Macromolecules, "Pathway and kinetics of cylinder-to-sphere order-order transition in block copolymers", 2000, 33, 3810-3817.

[19] M. Motomatsu, W. Mizutani, H. Tokumoto, Polymer, “Microphase domains of poly(styrene-block-ethylene/butylene-block-styrene) triblock copolymers studied by atomic force microscopy”, 1997, 98, 8, 1779-1997.

[20] T. Zhou, Z. Wu, Y. Li, J. Luo, Z. Chen, J. Xia, H. Liang, A. Zhang, Polymer, “Order-order, lattice disordering, and order-disorder transition in SEBS studied by two-dimensional correlation infrared spectroscopy, 2010, 51, 4249-4258.

[21] C. Peinado, T. Corrales, F. Catalina, S. Pedròn, V. R. S. Quiteria, M. D. Parellada, J. A. Barrio, D. Olmos, J. Gonzàlez-Benito, Polymer Degradation and Stability, “Effects of ozone in surface modification and thermal stability of SEBS block copolymers”, 2010, 95, 975-986.

[22] N. S. Allen, M. Edge, A. Wilkinson, C. M. Liauw, D. Mourelatou, J. Barrio, M. A. Martìnez-Zaporta, Polymer Degradation and Stability, “Degradation and stabilization of styrene-ethylene-butadiene-styrene (SEBS) block copolymer”, 2001, 71, 113-122.

[23] A. Pucci, D. Lorenzi, M.-B. Coltelli, G. Polimeni, E. Passaglia, Journal of Applied Polymer Science, “Controlled Degradation by Melt Processing with Oxygen or Peroxide of Ethylene/Propylene Copolymers”, 2004, 94, 372-381.

[24] S. Panteny, R. Stevens, C. R. Bowen, Ferroelectrics, “The frequency dependent permittivity and AC conductivity of random electrical networks”, 2005, 319, 199-208.